AIAA JOURNAL
Vol. 30, No. 5, May 1992

# Asymptotic Defect Boundary-Layer Theory Applied to Hypersonic Flows

B. Aupoix,* J. Ph. Brazier,† and J. Cousteix‡
*CERT/ONERA, 31055, Toulouse, France*

**For hypersonic re-entry flows, the bow shock wave upstream of the spacecraft is the cause of an inviscid vortical flow in the shock layer. Prandtl's equations are unable to cope with outer flow vorticity, whereas Van Dyke's matched asymptotic expansions approach no longer gives a good matching of the viscous and inviscid solutions when the boundary layer is thick. A new approach, using a defect formulation in the viscous region together with a matched asymptotic expansions technique, has been developed. The so-derived equations are consistent with Prandtl's or Van Dyke's equations. Fair predictions are achieved for incompressible flows with external vorticity only with second-order solutions because displacement effects have to be accounted for, whereas for hypersonic flows where displacement effects are weak, a good agreement with Navier-Stokes solutions is obtained with a first-order approach.**

## I. Introduction

THE boundary-layer equations were first derived by Prandtl using an order-of-magnitude approach. One of the drawbacks of Prandtl's equations is that they cannot account for normal gradients in the external flow. This has been the topic of a long debate in the fifties,[1-4] which led Van Dyke[5-8] to propose the use of matched asymptotic expansions as a tool to construct a boundary-layer theory. The key advantages of Van Dyke's approach is that, on the one hand, it gives a formalism to embed various supplementary phenomena in a general boundary-layer theory and that, on the other hand, not only the boundary-layer equations but also the matching relations between the viscous and inviscid solutions are so formally derived.

With this approach, Prandtl's equations are retrieved as first-order equations, whereas external flow gradients are accounted for only by the second-order solution, which is a perturbation of Prandtl's equations solution. Van Dyke has identified various second-order effects, i.e., displacement, external flow gradients, wall curvature, and rarefaction. He has also shown that displacement and external vorticity are strongly coupled.

Van Dyke's approach is based on asymptotic expansions when the characteristic Reynolds number tends toward infinity i.e., when the boundary layer is very thin. Therefore, Van Dyke assumed that the inviscid solution can be represented, in the boundary layer, by its Taylor expansion at the wall. Consequently, this approach gives a correct matching between the viscous and inviscid solutions only when the inviscid solution can be reduced to its Taylor expansion at the wall.

This is a severe drawback for hypersonic re-entry flows where Reynolds numbers are low so that thick boundary layers are encountered. The bow shock upstream of a blunt nose leads to a vortical inviscid flow over the body. This vorticity layer, usually called entropy layer, may be a region of nonconstant external flow vorticity that is gradually covered by the boundary layer. Hence, no correct matching of the viscous and inviscid solutions and also no correct prediction of the influence of the external vorticity on the wall heat flux or the skin friction can be achieved with Van Dyke's second-order approach.

## II. Defect Approach

### A. Motivations

To be able to account for arbitrary inviscid flows in the boundary-layer region, a defect approach has been proposed. Such an approach ensures a correct matching of the viscous and inviscid solutions and has been already used in viscous-inviscid interaction problems (see, e.g., Refs. 9 and 10).

Van Dyke has brought into evidence that external vorticity and displacement effects are both second-order effects and are strongly coupled. It is a priori difficult to take into account these effects without using a second-order approach. However, concerning re-entry flows, displacement effects are weak since the wall is cold so that the external vorticity effect can be considered solely, with the defect approach, in the framework of a first-order approximation.

The matched asymptotic expansions approach is still used to derive the governing equations as it is a very powerful tool.

Only steady, two-dimensional, laminar, compressible, perfect gas flows will be addressed here.

### B. Basic Equations

The basic equations are the Navier-Stokes equations, which are written in dimensionless form with reference to the upstream velocity $U_\infty$, upstream density $\rho_\infty$, a reference length $R_0$ such as the nose radius, a reference temperature $T_0 = U_\infty^2/c_p$, and a reference viscosity $\mu_0 = \mu(T_0)$.

A convenient coordinate system, linked to the body surface, is used. At least in the wall region the system is orthogonal, with the dimensionless abscissa along the body $\xi$ and the dimensionless distance along the wall normal $\eta$. The continuity, longitudinal and normal momentum, energy, and state equations read

$$\frac{\partial}{\partial \xi}(h_3 \rho u) + \frac{\partial}{\partial \eta}(h_1 h_3 \rho v) = 0 \tag{1}$$

Presented as Paper 91-0026 at the AIAA 29th Aerospace Sciences Meeting, Reno, NV, Jan. 7-10, 1991; received Feb. 26, 1991; revision received July 24, 1991; accepted for publication July 26, 1991. 

*Research Engineer, Department of Aerothermodynamics, 2, Avenue E. Belin, BP 4025. Member AIAA.

†Research Engineer, Department of Aerothermodynamics, 2, Avenue E. Belin, BP 4025.

‡Head of Department, Department of Aerothermodynamics, 2, Avenue E. Belin, BP 4025. Senior Member AIAA.

$$\rho u\frac{\partial u}{\partial \xi}+\rho v\frac{\partial (h_1 u)}{\partial \eta}=-\frac{\partial p}{\partial \xi}$$
$$+\frac{1}{h_1 h_3}\frac{\partial}{\partial \eta}\left\{\frac{\mu}{Re}h_1 h_3\left[\frac{\partial v}{\partial \xi}+h_1^2\frac{\partial}{\partial \eta}\left(\frac{u}{h_1}\right)\right]\right\}$$
$$+\frac{\partial}{\partial \xi}\left[\frac{2}{3}\frac{\mu}{Re}\left(\frac{2v}{h_1}\frac{\partial h_1}{\partial \eta}+\frac{2}{h_1}\frac{\partial u}{\partial \xi}-\frac{\partial v}{\partial \eta}-\frac{v}{h_3}\frac{\partial h_3}{\partial \eta}\right.\right.$$
$$\left.\left.-\frac{u}{h_1 h_3}\frac{\partial h_3}{\partial \xi}\right)\right]+\frac{2\mu}{Re}\frac{1}{h_3}\frac{\partial h_3}{\partial \xi}\left[\frac{v}{h_1}\frac{\partial h_1}{\partial \eta}-\frac{v}{h_3}\frac{\partial h_3}{\partial \eta}\right.$$
$$\left.+\frac{1}{h_1}\frac{\partial u}{\partial \xi}-\frac{u}{h_1 h_3}\frac{\partial h_3}{\partial \xi}\right] \tag{2}$$

$$\rho u\frac{1}{h_1}\frac{\partial v}{\partial \xi}+\rho v\frac{\partial v}{\partial \eta}-\rho u^2\frac{1}{h_1}\frac{\partial h_1}{\partial \eta}=-\frac{\partial p}{\partial \eta}$$
$$+\frac{1}{h_1 h_3}\frac{\partial}{\partial \xi}\left\{\frac{\mu}{Re}h_3\left[\frac{1}{h_1}\frac{\partial v}{\partial \xi}+h_1\frac{\partial}{\partial \eta}\left(\frac{u}{h_1}\right)\right]\right\}$$
$$+\frac{\partial}{\partial \eta}\left[\frac{2}{3}\frac{\mu}{Re}\left(2\frac{\partial v}{\partial \eta}-\frac{1}{h_1}\frac{\partial u}{\partial \xi}-\frac{v}{h_1}\frac{\partial h_1}{\partial \eta}\right)\right]$$
$$+\frac{2\mu}{Re}\frac{1}{h_3}\frac{\partial h_3}{\partial \eta}\left[\frac{\partial v}{\partial \eta}-\frac{u}{h_1 h_3}\frac{\partial h_3}{\partial \xi}-\frac{v}{h_3}\frac{\partial h_3}{\partial \eta}\right]$$
$$+\frac{2\mu}{Re}\frac{1}{h_1}\frac{\partial h_1}{\partial \eta}\left[\frac{\partial v}{\partial \eta}-\frac{1}{h_1}\frac{\partial u}{\partial \xi}-\frac{v}{h_1}\frac{\partial h_1}{\partial \eta}\right] \tag{3}$$

$$\rho u\frac{1}{h_1}\frac{\partial h}{\partial \xi}+\rho v\frac{\partial h}{\partial \eta}=\frac{u}{h_1}\frac{\partial p}{\partial \xi}+v\frac{\partial p}{\partial \eta}$$
$$+\frac{1}{h_1 h_3}\frac{\partial}{\partial \xi}\left[\frac{\mu}{Pr\,Re}\frac{h_3}{h_1}\frac{\partial T}{\partial \xi}\right]+\frac{1}{h_1 h_3}\frac{\partial}{\partial \eta}\left[\frac{\mu}{Pr\,Re}h_1 h_3\frac{\partial T}{\partial \eta}\right]$$
$$+\frac{\mu}{Re}\left\{2\left(\frac{1}{h_1}\frac{\partial u}{\partial \xi}+\frac{v}{h_1}\frac{\partial h_1}{\partial \eta}\right)^2+2\left(\frac{\partial v}{\partial \eta}\right)^2\right.$$
$$+2\left(\frac{u}{h_1 h_3}\frac{\partial h_3}{\partial \xi}+\frac{v}{h_3}\frac{\partial h_3}{\partial \eta}\right)^2+\left[\frac{1}{h_1}\frac{\partial v}{\partial \xi}+h_1\frac{\partial}{\partial \eta}\left(\frac{u}{h_1}\right)\right]^2$$
$$\left.-\frac{2}{3}\left(\frac{1}{h_1}\frac{\partial u}{\partial \xi}+\frac{\partial v}{\partial \eta}+\frac{u}{h_1 h_3}\frac{\partial h_3}{\partial \xi}+\frac{v}{h_1}\frac{\partial h_1}{\partial \eta}+\frac{v}{h_3}\frac{\partial h_3}{\partial \eta}\right)^2\right\} \tag{4}$$

$$p=\frac{\gamma-1}{\gamma}\rho T \tag{5}$$

where $Re=(\rho_\infty U_\infty R_0)/\mu_0$ and $Pr=\mu c_p/k$ are the Reynolds and Prandtl numbers, respectively. These equations have been written using Stokes hypothesis, i.e., $3\lambda+2\mu=0$. In fact, Van Dyke[7] has shown that the second viscosity coefficient $\lambda$ only appears in third-order equations.

For an axisymmetric body, the metric coefficients read

$$h_1=1+\frac{\eta}{R},\qquad h_3=r+\eta\cos\alpha \tag{6}$$

where $R$ and $r$ are the longitudinal and transverse curvature radii, respectively, and $\alpha$ the angle between the wall tangent and the symmetry axis.

### C. Defect Variables

In the wall region, equations are sought not for the physical variables but for the difference with the inviscid solution. Defect variables (labeled with a subscript $D$) are defined with respect to the inviscid solution (labeled with a subscript $E$) as

$$u=u_E+u_D,\qquad v=v_E+v_D-v_E(\xi,0)$$
$$p=p_E+p_D,\qquad T=T_E+T_D,\qquad \rho=\rho_E+\rho_D \tag{7}$$

where the normal velocity component is shifted to ensure that $v_D(\xi,0)=0$.

### D. Asymptotic Expansions

As in Van Dyke's approach, approximations of the Navier-Stokes equations are sought, on the one hand, for the outer region where viscous effects are weak, i.e., far from the wall, and, on the other hand, for the inner region near the wall where viscous effects are important. Both solutions are defined over the whole domain but are valid only in a restricted zone. The analysis is similar to Van Dyke's: solutions are looked for as expansions in terms of a small parameter

$$\epsilon=\frac{1}{\sqrt{Re}}=\frac{1}{\sqrt{(\rho_\infty U_\infty R_0)/\mu_0}}$$

In the inner region, a magnified normal coordinate $\bar{\eta}=\eta/\epsilon$ is used. As usual, capital letters are used for outer variables, small letters for inner variables. The outer expansions read

$$\begin{aligned}
u_E(\xi,\eta)&=U_1(\xi,\eta)+\epsilon U_2(\xi,\eta)+\cdots\\
v_E(\xi,\eta)&=V_1(\xi,\eta)+\epsilon V_2(\xi,\eta)+\cdots\\
p_E(\xi,\eta)&=P_1(\xi,\eta)+\epsilon P_2(\xi,\eta)+\cdots\\
\rho_E(\xi,\eta)&=R_1(\xi,\eta)+\epsilon R_2(\xi,\eta)+\cdots\\
T_E(\xi,\eta)&=T_1(\xi,\eta)+\epsilon T_2(\xi,\eta)+\cdots
\end{aligned} \tag{8}$$

whereas the inner expansions

$$\begin{aligned}
u_D(\xi,\eta)&=u_1(\xi,\bar{\eta})+\epsilon u_2(\xi,\bar{\eta})+\cdots\\
v_D(\xi,\eta)&=\epsilon\bar{v}_1(\xi,\bar{\eta})+\epsilon^2\bar{v}_2(\xi,\bar{\eta})+\cdots\\
p_D(\xi,\eta)&=p_1(\xi,\bar{\eta})+\epsilon p_2(\xi,\bar{\eta})+\cdots\\
\rho_D(\xi,\eta)&=\rho_1(\xi,\bar{\eta})+\epsilon\rho_2(\xi,\bar{\eta})+\cdots\\
T_D(\xi,\eta)&=t_1(\xi,\bar{\eta})+\epsilon t_2(\xi,\bar{\eta})+\cdots
\end{aligned} \tag{9}$$

bring into evidence the classical shift in the normal velocity component expansion to avoid the degeneracy of the inner continuity equation.

Special attention has to be paid to the order-of-magnitude analysis of the external flow quantities in the inner region. For example, the normal velocity component can be expanded as

$$V_1(\xi,\eta)-V_1(\xi,0)=\epsilon\tilde{V}_1(\xi,\eta)$$

and other quantities such as the longitudinal velocity component, the pressure, or the density and their derivatives are of order unity.

### E. Flow Equations

#### 1. *Outer Region*

Expansion (8) is brought into the Navier-Stokes equations [Eqs. (1-5)] and like powers of $\epsilon$ are equated. This leads to the Euler's equations as first-order equations and linearized Euler equations for small perturbations as second-order equations, as with Van Dyke's approach.

#### 2. *Inner Region*

The derivation procedure for the inner region equations is more complex. In the Navier-Stokes equations [Eqs. (1-5)], the variables are first expressed in terms of external and defect variables according to Eqs. (7). The inner [Eqs. (9)] and outer [Eqs. (8)] expansions are then introduced and the previously derived first- and second-order Euler's equations are sub-

tracted. Like powers of $\epsilon$ are then equated and equations are written in terms of external variables $(\xi,\eta=\epsilon\bar{\eta})$ with

$$v_1(\xi,\eta)=\epsilon\bar{v}_1(\xi,\bar{\eta})$$

The first-order equations read

$$\frac{\partial}{\partial\xi}\left[r\rho_1U_1+r(R_1+\rho_1)u_1\right]+\frac{\partial}{\partial\eta}\left[r\rho_1(V_1+v_1)\right]+rR_1\frac{\partial v_1}{\partial\eta}=0 \tag{10}$$

$$(R_1+\rho_1)(U_1+u_1)\frac{\partial u_1}{\partial\xi}+\left[\rho_1U_1+(R_1+\rho_1)u_1\right]\frac{\partial U_1}{\partial\xi}$$
$$+(R_1+\rho_1)(V_1+v_1)\frac{\partial u_1}{\partial\eta}=-\frac{\partial p_1}{\partial\xi}+\frac{1}{Re}\frac{\partial}{\partial\eta}\left(\mu_1\frac{\partial u_1}{\partial\eta}\right) \tag{11}$$

$$0=-\frac{\partial p_1}{\partial\eta} \tag{12}$$

$$(R_1+\rho_1)(U_1+u_1)\frac{\partial t_1}{\partial\xi}+\left[\rho_1U_1+(R_1+\rho_1)u_1\right]\frac{\partial T_1}{\partial\xi}$$
$$+(R_1+\rho_1)(V_1+v_1)\frac{\partial t_1}{\partial\eta}=u_1\frac{\partial P_1}{\partial\xi}+(U_1+u_1)\frac{\partial p_1}{\partial\xi}$$
$$+\frac{\partial}{\partial\eta}\left(\frac{\mu_1}{Pr\,Re}\frac{\partial t_1}{\partial\eta}\right)+\frac{\mu_1}{Re}\left(\frac{\partial u_1}{\partial\eta}\right)^2 \tag{13}$$

$$p_1=\frac{\gamma-1}{\gamma}\left[\rho_1T_1+(R_1+\rho_1)t_1\right] \tag{14}$$

For a plane surface, second-order equations are linearized forms of Eqs. (10–14) for small perturbations; otherwise, they also include extra terms due to wall curvature, which are still second-order effects since the metric coefficients (6) can be expressed, in the inner region, as

$$h_1=1+\epsilon\frac{\bar{\eta}}{R},\qquad h_3=r+\epsilon\bar{\eta}\cos\alpha$$

### F. Matching Conditions

One of the key advantages of using a matched asymptotic expansions approach is that it gives a formalism to express matching between the inner and outer solutions.

Matching conditions are obtained as Van Dyke by stating that the $m$-term inner expansion of the $n$-term outer expansion is equal to the $n$-term outer expansion of the $m$-term inner expansion. This leads to the following relations

$$\lim_{\bar{\eta}\to\infty}u_1=0,\quad\lim_{\bar{\eta}\to\infty}p_1=0,\quad\lim_{\bar{\eta}\to\infty}t_1=0,\quad\lim_{\bar{\eta}\to\infty}\rho_1=0$$

for the first-order solution and

$$\lim_{\bar{\eta}\to\infty}u_2=0,\quad\lim_{\bar{\eta}\to\infty}p_2=0,\quad\lim_{\bar{\eta}\to\infty}t_2=0,\quad\lim_{\bar{\eta}\to\infty}\rho_2=0$$

for the second-order solution. The normal velocity component study leads to different conclusions, thanks to the shifted inner expansion

$$V_1(\xi,0)=0,\qquad V_2(\xi,0)=\lim_{\bar{\eta}\to\infty}\bar{v}_1(\xi,\bar{\eta})$$

i.e., the first-order outer equations must satisfy the slip condition at the wall while the displacement effect of the first-order boundary layer is accounted for in the second-order outer flow computation as a wall injection.

With these matching conditions, Eq. (12) reduces to $p_1=0$ throughout the inner region, i.e., the pressure in the boundary layer is everywhere equal to the inviscid pressure. This is still true for the second-order solution if there are no curvature effects.

### G. Wall Conditions

The wall conditions for the inner solutions are deduced from the Navier-Stokes equations wall conditions. Rarefaction effects, i.e., slip velocity and temperature jump, are not accounted for here. With a prescribed wall temperature, the wall conditions read

$$u=u_E+u_D=U_1+u_1+\epsilon(U_2+u_2)=0$$
$$v=v_E-v_E(\xi,0)+v_D=\epsilon\bar{v}_1+\epsilon^2\bar{v}_2=0$$
$$T=T_E+T_D=T_1+t_1+\epsilon(T_2+t_2)=T_w$$

hence,

$$u_1(\xi,0)=-U_1(\xi,0),\qquad u_2(\xi,0)=-U_2(\xi,0)$$
$$v_1(\xi,0)=0,\qquad v_2(\xi,0)=0$$
$$t_1(\xi,0)=T_w-T_1(\xi,0),\qquad t_2(\xi,0)=-T_2(\xi,0)$$

### H. Discussion

Because of the matching conditions, the inner and outer solutions are hierarchized as with Van Dyke's approach: the outer (Euler) first-order equations are first solved with a slip condition at the wall, then the inner (boundary-layer) first-order equations with imposed inviscid flow velocity and pressure distributions, then the second-order outer solution is sought, which accounts for the boundary-layer displacement, and, finally, the second-order inner solution.

The defect inner equations have the same mathematical properties as Van Dyke's equations. They form a set of parabolic equations and can be solved with a space-marching procedure. The simplicity of the Euler plus boundary-layer approach is thus preserved.

The defect inner equations are consistent with those obtained by Van Dyke as they only differ by terms that are of higher order in Van Dyke's analysis. If the flow over a plane surface is considered, inner and outer first-order equations can be combined to form equations for the physical variables in the inner region

$$\frac{\partial(\rho u)}{\partial\xi}+\frac{\partial(\rho v)}{\partial\eta}=v_D\frac{\partial\rho_E}{\partial\eta}$$
$$\rho u\frac{\partial u}{\partial\xi}+\rho v\frac{\partial u}{\partial\eta}-(\rho v-\rho_Ev_E)\frac{\partial u_E}{\partial\eta}=-\frac{\partial p}{\partial\xi}+\frac{1}{Re}\frac{\partial}{\partial\eta}\left[\mu\frac{\partial u_D}{\partial\eta}\right]$$
$$\rho u\frac{\partial T}{\partial\xi}+\rho v\frac{\partial T}{\partial\eta}-(\rho v-\rho_Ev_E)\frac{\partial T_E}{\partial\eta}=u\frac{\partial p}{\partial\xi}+v_E\frac{\partial p}{\partial\eta}$$
$$+\frac{\partial}{\partial\eta}\left[\frac{\mu}{Pr\,Re}\frac{\partial T_D}{\partial\eta}\right]+\frac{\mu}{Re}\left(\frac{\partial u_D}{\partial\eta}\right)^2$$
$$p=\frac{\gamma-1}{\gamma}\rho T$$

which reduce to Prandtl's equations only when the inviscid flow is constant along the wall normals.

Rarefaction effects, when considered, as well as wall curvature and displacement are still second-order effects as with Van Dyke's approach. The improvement of this approach is that external flow variations are now accounted for in the first-order inner solution and that a good matching of the inner and outer solutions is ensured.

## III. Application to Flow Calculations

No self-similar solutions have been found when the inviscid flow varies along the normal. Only local similarity has been investigated for a constant shear flow past a flat plate, as well as with Van Dyke's approach[4] as with the defect approach.[11,12]

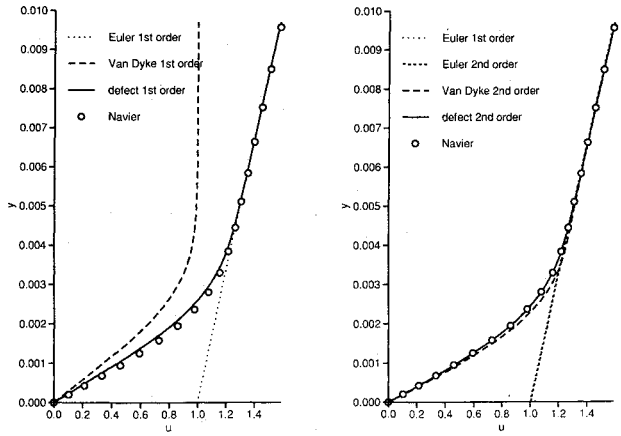


**Fig. 1 First- and second-order velocity profiles for a constant shear flow: $x = 0.9$.**

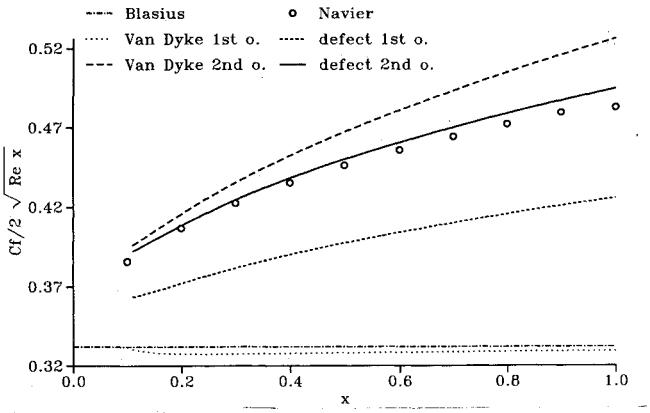


**Fig. 2 Skin-friction coefficient distributions for a constant shear flow.**

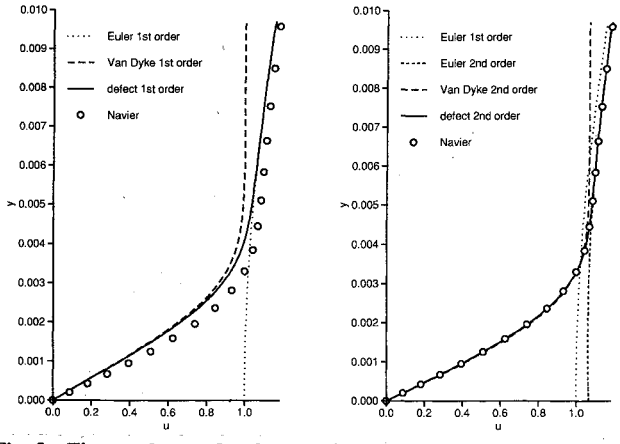


**Fig. 3 First- and second-order velocity profiles for a hyperbolic shear flow: $x = 0.9$.**

Data are needed in order to validate the defect approach and to compare it with the classical Van Dyke's approach. As experiments in laminar flow with significant external vorticity effects are rare, numerical experiments have been used. Navier-Stokes solutions[13,14] have been run to provide reference solutions. The same cases have also been computed with the usual Euler plus boundary-layer approach using both Van Dyke's and defect formulations.

### A. Incompressible Sheared Flow over a Flat Plate

To first investigate the effect of external velocity gradients, first- and second-order solutions for an incompressible, parallel, laminar, sheared flow over a flat plate have been looked at. Since a Cartesian reference frame is used here, $x$ and $y$ indicate distances along and normal to the plate, respectively. Dimensionless variables, with respect to the incoming velocity on the plate and to the plate length, are used.

The incoming flow is

$$U_1 = U_1(y), \qquad V_1 = 0, \qquad P_1 = \text{constant}$$

which is solution of the Euler's equations. Various shear distributions have been investigated.[11] The reference Reynolds number, based on the plate length and $U_1(0)$, is $10^6$.

A first example is a constant shear flow $U_1 = 1 + \omega y$. A dimensionless shear $\omega$ equal to 60 has been used. First- and second-order velocity profiles are shown in Fig. 1; the evolution of the skin-friction coefficient is plotted in Fig. 2.

The defect approach provides a correct matching with the outer solution in contrast with Van Dyke's solution. Hence, it gives a better agreement with the Navier-Stokes computations. The second-order outer solution is, in this case, very close to the first-order one. As the shear is constant, a good matching is thus achieved with both second-order approaches. However, Van Dyke's approach then overpredicts the skin friction and good prediction is achieved only with the second-order defect approach.

The second example is an incoming hyperbolic shear flow

$$U_1 = \sqrt{1 + 3600\,y^2}$$

i.e., the shear is null at the wall and increases up to a value of 60. First- and second-order velocity profiles are shown in Fig. 3; the evolution of the skin-friction coefficient is plotted in Fig. 4.

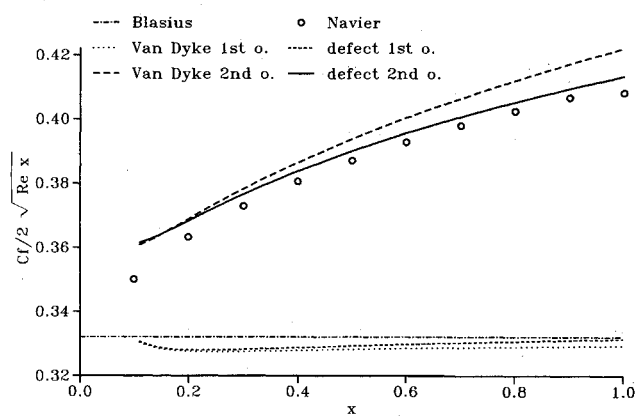


**Fig. 4 Skin-friction coefficient distributions for a hyperbolic shear flow.**

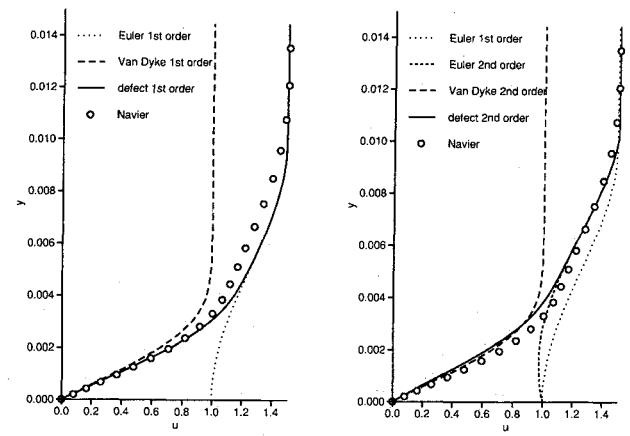


**Fig. 5 First- and second-order velocity profiles for a sinusoidal shear flow: $x = 0.9$.**

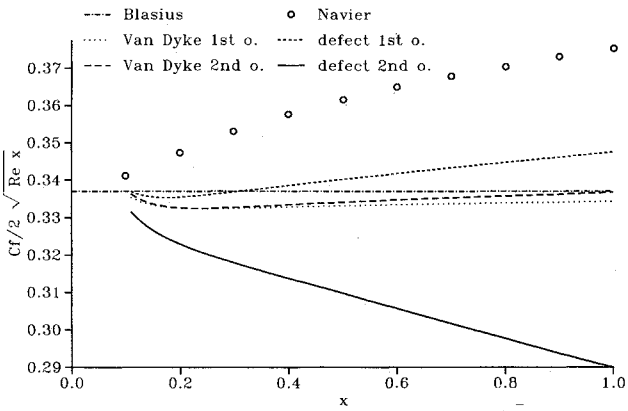


**Fig. 6 Skin-friction coefficient distributions for a sinusoidal shear flow.**

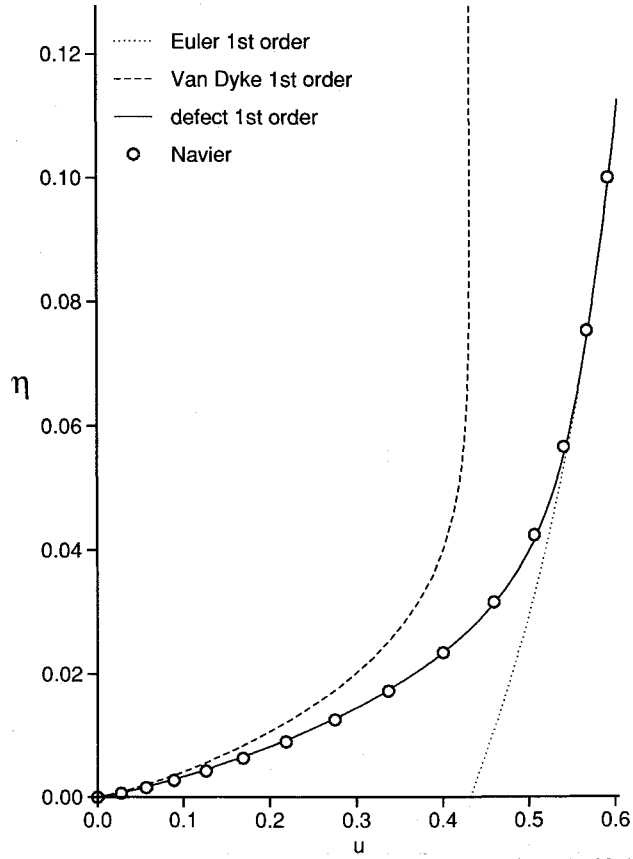


**Fig. 7 Longitudinal velocity profiles on the hyperboloid: $M = 23.4$; $T_w = 1500$ K; $\xi = 4$.**

The outer vorticity is null at the wall. This leads to a failure of Van Dyke's approach, which is no longer able to give a correct matching, neither with first- nor with second-order solutions. The change between first- and second-order outer solutions is obvious, as well for the velocity as for the vorticity. The first- and second-order defect approaches provide, of course, a good matching. The second-order solution is in good agreement with the Navier-Stokes solution. The influence of the inviscid shear is weak since it varies from 0 at the wall to 17 at the outer edge of the boundary layer ($y \sim 0.005$), whereas the displacement effect is important. Hence, both Van Dyke's and defect second-order approaches give fair predictions of the skin friction.

The last example shows the limit of the boundary-layer approach. The incoming flow has now a sinusoidal velocity profile

$$U_1 = 1 + \tfrac{1}{2} \sin^2(50\pi y), \qquad y \le 0.01$$

$$U_1 = 1.5, \qquad y \ge 0.01$$

where the incoming shear is again null on the plate and has a maximum value $25\pi$. Velocity profiles are shown in Fig. 5; the evolution of the skin-friction coefficient is plotted in Fig. 6.

Here again, as the shear is not constant through the boundary layer, Van Dyke's solution is unable to provide a correct matching. The defect approach yields a good matching but fails to reproduce the Navier-Stokes solution. As the velocity profile is poorly predicted in the wall region, the skin friction is underestimated. Both the second-order theories cannot deal with the non-negligible viscous effects occuring in the outer region above the boundary layer. In this case, the inviscid profile is strongly curved and the curvature variations are represented by the third-order $y$ derivative, which is included only in the fourth-order perturbation term. Thus, a fourth-order expansion at least should be necessary to obtain a good approximation of the Navier-Stokes solution.

The previously presented applications show that the defect approach greatly improves the matching and is able to give fair predictions in situations where the Euler plus boundary-layer approach makes sense, but as concerns incompressible flows, it requires the second-order approach to correctly account for the external vorticity since its effect is coupled with the displacement effect.

### B. Hypersonic Re-Entry Flow over an Axisymmetric Hyperboloid

The flow over the axisymmetric hyperboloid at 0-deg incidence, which is supposed to mimic the Space Shuttle windward symmetry plane,[15,16] has been used as a test case. Various altitudes have been investigated.[11] Only first-order solutions are presented as no second-order inviscid flow computations have been performed yet. No comparison with flight data can be done since real gas effects are not accounted for. The viscosity is taken from the Sutherland law and the Prandtl number is assumed to be constant.

In Van Dyke's approach, the stagnation point solution is obtained with the help of the Levy-Lees-Dorodnitsyn transfor-

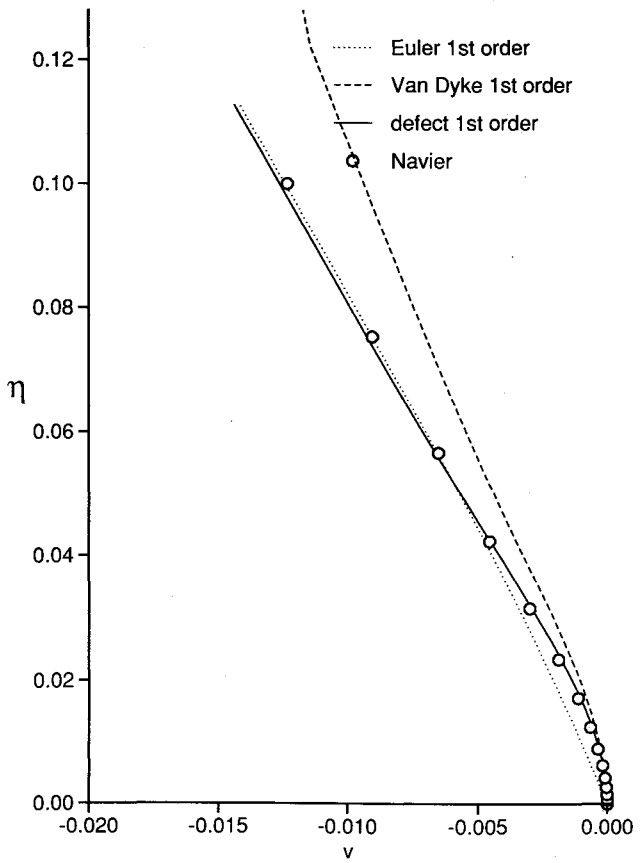


**Fig. 8 Normal velocity profiles on the hyperboloid: $M = 23.4$; $T_w = 1500$ K; $\xi = 4$.**

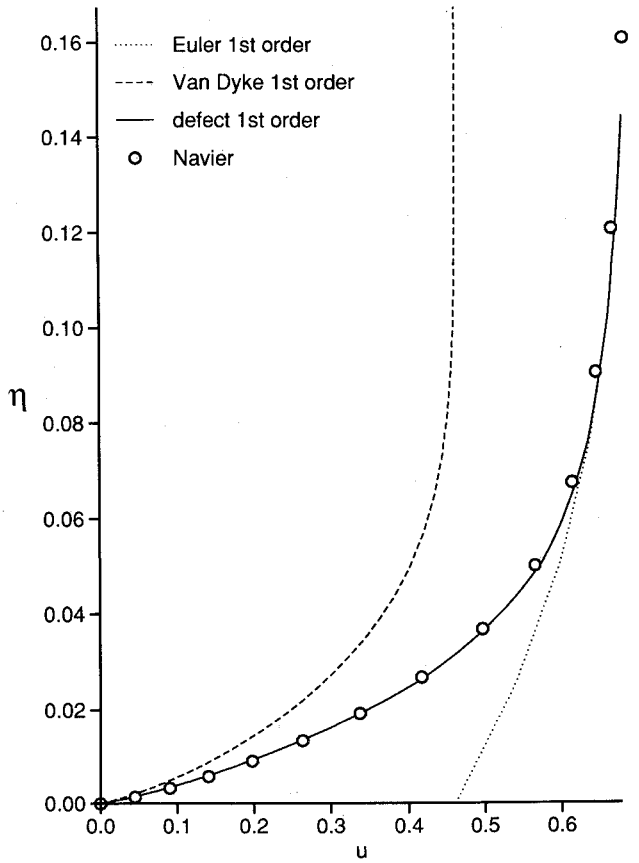


**Fig. 9 Longitudinal velocity profiles on the hyperboloid: $M = 23.4$; $T_w = 1500$ K; $\xi = 9.5$.**

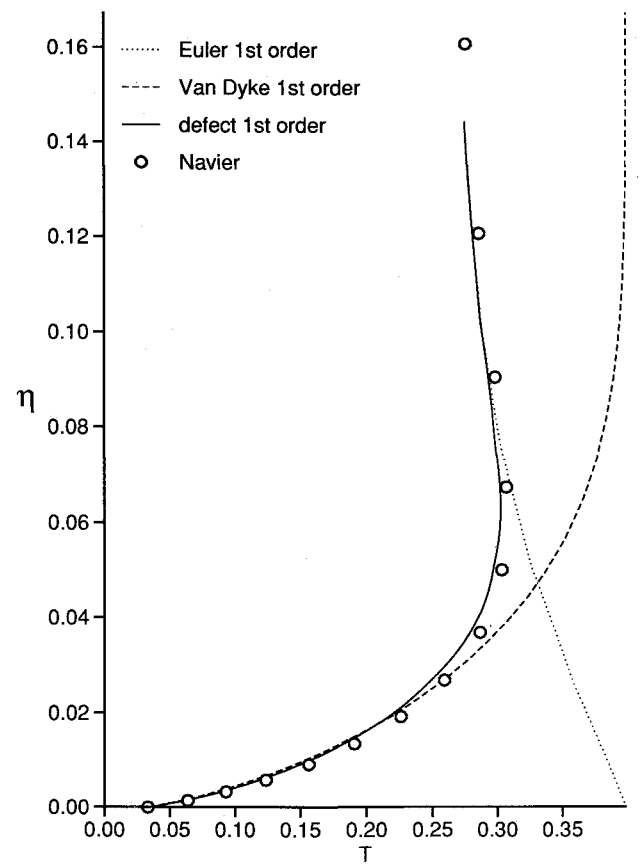


**Fig. 10 Temperature profiles on the hyperboloid: $M = 23.4$; $T_w = 1500$ K; $\xi = 9.5$.**

mation, whereas in the defect approach, polynomial expansions with respect to the curvilinear coordinate $\xi$ are used, as in Van Dyke.[7]

Only one set of results will be presented here. It corresponds to the following conditions of the STS-2 re-entry

$$t = 650 \text{ s}, \quad Z = 71.29 \text{ km}, \quad U_\infty = 6730 \text{ m s}^{-1}$$

$$\rho_\infty = 6.824 \times 10^{-5} \text{ kg m}^{-3}, \quad p_\infty = 6.91 \text{ Pa}, \quad T_\infty = 205 \text{ K}$$

$$M_\infty = 23.4, \quad R_0 = 1.253 \text{ m}, \quad \alpha = 40.2 \text{ deg}$$

where $\alpha$ is half the hyperboloid asymptotes angle, and the wall temperature has been fixed to 1500 K. This case corresponds to a Reynolds number based on upstream conditions and nose radius of 1866 or a small parameter $\epsilon$ of 0.0231, i.e., a typically low Reynolds number flow.

Euler solutions are now obtained with a code developed at ONERA.[17] Boundary-layer profiles are displayed in Figs. 7–10 for two locations along the body. Longitudinal velocity profiles are plotted in Figs. 7 and 9. The inviscid flow shear is maximum at the wall and decreases above. Only the defect approach can match the inviscid solution with a first-order approach. The agreement with the Navier-Stokes solution is fair. Even with a second-order approach, no correct matching could be achieved with Van Dyke's approach. Moreover, Adams[18] has shown that such a decreasing shear can lead to severe failures of Van Dyke's second-order approach since the external shear is then overestimated.

The velocity component normal to the wall is plotted in Fig. 8. As expected for hypersonic re-entry flows, displacement effect seems to be weak as the wall temperature is low so that there is little difference between the Euler and the Navier-

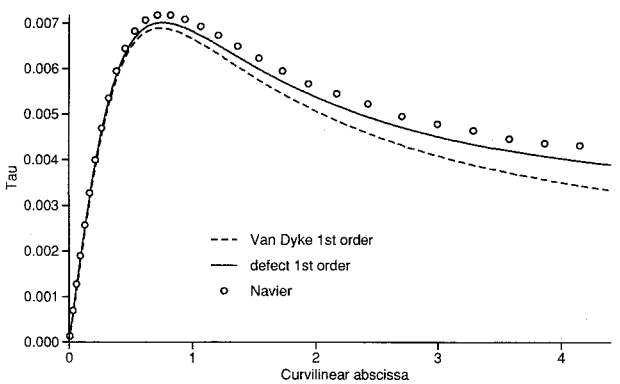


**Fig. 11 Skin-friction predictions on the hyperboloid: $M = 23.4$; $T_w = 1500$ K—nose region.**

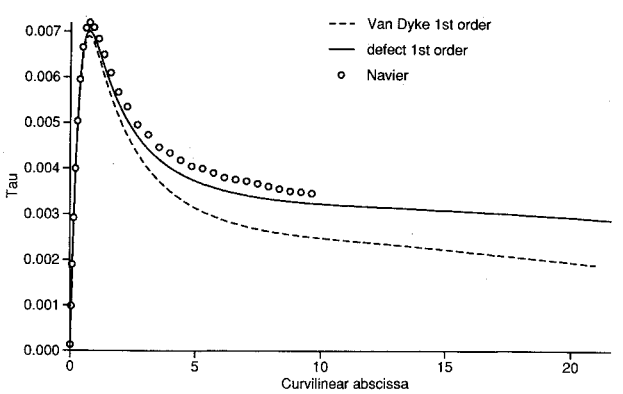


**Fig. 12 Skin-friction predictions on the hyperboloid: $M = 23.4$; $T_w = 1500$ K—complete body.**

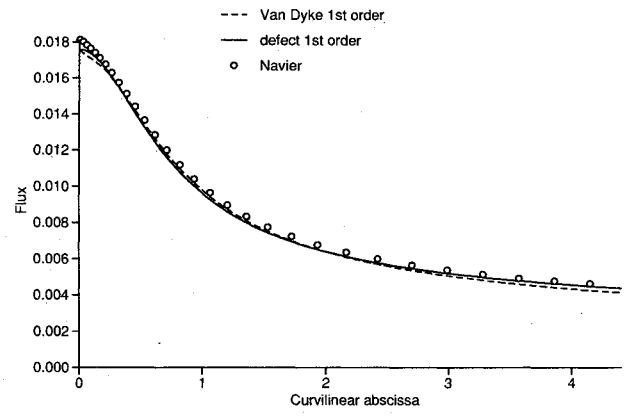


**Fig. 13 Wall heat flux predictions on the hyperboloid: $M = 23.4$; $T_w = 1500$ K—nose region.**

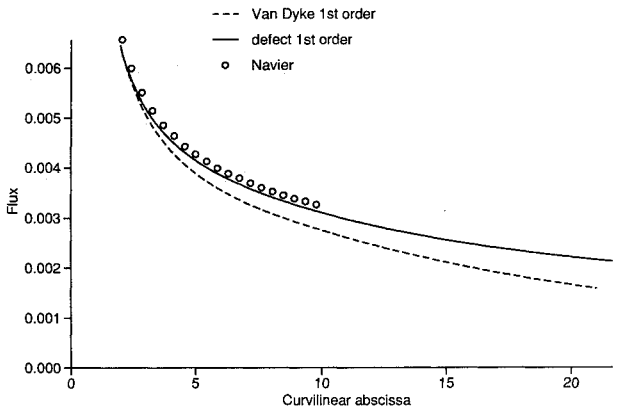


**Fig. 14 Wall heat flux predictions on the hyperboloid: $M = 23.4$; $T_w = 1500$ K—complete body.**

Stokes distributions. Van Dyke's solution overestimates the normal velocity mainly because it overestimates the normal velocity gradient. With Van Dyke's approach, the longitudinal velocity component and the density must tend outside the boundary layer toward the inviscid wall value. Hence, through the continuity equation, the normal velocity gradient at the outer edge of the boundary layer is poorly predicted.

The temperature profile is displayed in Fig. 10. Since the stagnation enthalpy is constant in absence of viscous effects, the temperature gradient of the inviscid solution is due to the longitudinal velocity gradient. Here again, better predictions are achieved using the defect approach.

Evolutions of the skin friction along the hyperboloid are plotted in Figs. 11 and 12. No Navier-Stokes solution over the complete body is presently available for comparison. It is clear, however, that the defect approach greatly improves the prediction. Some discrepancies are still observed, which may be corrected by a second-order approach. The wall heat flux evolutions are plotted in Figs. 13 and 14. Here again, the use of the defect approach greatly improves the prediction. As usual, the Prandtl's equations underestimate both the skin friction and the wall heat flux and more the skin friction than the wall heat flux.

Tests for other points along the STS-2 re-entry trajectory confirm this analysis.[11,19] The defect approach greatly improves the prediction but still slightly underestimates both the skin friction and the heat flux. Significant departures between the Navier-Stokes and first-order defect solutions are observed only at very high altitudes when the boundary layer occupies all of the shock layer.

## Conclusions

The defect approach has been proposed as a way to derive boundary-layer equations from the Navier-Stokes equations, taking advantage of the matched asymptotic expansions methodology while taking into account variations of the inviscid solution in the boundary-layer region to ensure a correct matching.

A set of equations consistent with the one obtained by Van Dyke is so deduced. External flow gradients are now first-order effects. In the present version, curvature is still a second-order effect but could also be dealt with as a first-order effect.

For incompressible flows, in which displacement effects are important, and as displacement is coupled with external velocity gradient, a correct prediction of flows with external vorticity can be achieved only by using a second-order approach.

For re-entry flows where displacement effects are weak, first-order solutions already give very nice results.

In all cases, a fair matching of the inviscid and the viscous solutions is ensured.

As the so-obtained equations are similar to Van Dyke's equations, they have the same mathematical properties, i.e., they are parabolic and can be solved easily with the help of a marching procedure.

This approach, originally derived for re-entry flows, has other application fields. All flows with significant second-order effects, such as wall curvature, or vortical flows, such as supersonic flows behind curved shocks, or external flows with any gradient, such as stagnation enthalpy gradient for turbomachinery applications, could be considered. Extensions to real gas flows, turbulent flows, and three-dimensional flows are in progress.

## References

[1]Glauert, M. B., "The Boundary Layer in Simple Shear Flow Past a Flat Plate," *Journal of the Aeronautical Sciences—Reader's Forum,* Vol. 24, Nov. 1955, pp. 848–849.

[2]Li, T. Y., "Simple Shear Flow Past a Flat Plate in an Incompressible Fluid of Small Viscosity," *Journal of the Aeronautical Sciences—Reader's Forum,* Vol. 22, Sept. 1955, pp. 651, 652.

[3]Li, T. Y., "Effects of Free-Stream Vorticity on the Behavior of a Viscous Boundary Layer," *Journal of the Aeronautical Sciences—Reader's Forum,* Vol. 23, Dec. 1956, pp. 1128–1129.

[4]Murray, J. D., "The Boundary Layer on a Flat Plate in a Stream with Uniform Shear," *Journal of Fluid Mechanics,* Vol. 11, 1961, pp. 309–316.

[5]Van Dyke, M., "Higher Approximations in Boundary-Layer Theory—Part 1: General Analysis," *Journal of Fluid Mechanics,* Vol. 14, 1962, pp. 161–177.

[6]Van Dyke, M., "Higher Approximations in Boundary-Layer Theory—Part 2: Application to Leading Edges," *Journal of Fluid Mechanics,* Vol. 14, 1962, pp. 481–495.

[7]Van Dyke, M., "Second-Order Compressible Boundary Layer Theory with Application to Blunt Bodies in Hypersonic Flow," *Hypersonic Flow Research,* Vol. 7, edited by F. R. Riddell, Academic, 1962, pp. 37–76.

[8]Van Dyke, M., "Higher-Order Boundary-Layer Theory," *Annual Review of Fluid Mechanics,* 1969, pp. 265–292.

[9]East, L. F., "A Representation of Second-Order Boundary Layer Effects in the Momentum Integral Equation and in Viscous-Inviscid Interactions," Royal Aircraft Establishment, Farnborough, Hants, England, UK, TR 81002, Jan. 1981.

[10]Le Balleur, J. C., "Calcul des Écoulements à Forte Interaction Visqueuse au Moyen de Méthodes de Couplage," *Computation of Viscous-Inviscid Interactions,* AGARD CP 291, U.S. Air Force Academy, Colorado Springs, CO, Sept.-Oct. 1980.

[11]Brazier, J.-Ph., "Etude Asymptotique des Équations de Couche Limite en Formulation Déficitaire," Ph.D. Dissertation, Ecole Nationale Supérieure de l'Aéronautique et de l'Espace, Toulouse, France, June 1990.

[12]Brazier, J.-Ph., Aupoix, B., and Cousteix, J., "Etude Asymptotique de la Couche Limite en Formulation Déficitaire," *Compte-Rendus de l'Académie des Sciences—t. 310 Série II,* 1990, pp. 1583–1588.

[13]Gendre, P., "Calcul d'écoulements Turbulents Décollés par résolution des Equations de Navier-Stokes," Ph.D. Dissertation, Ecole Nationale Supérieure de l'Aéronautique et de l'Espace, Tou-

louse, France, March 1990.

[14]Lafon, A., "Calcul d'écoulements Visqueux Hypersoniques," ONERA, Rept. RT 32/5005.22, March 1990.

[15]Shinn, J., Moss, J. N., and Simmonds, A. L., "Viscous Shock-Layer Heating Analysis for the Shuttle Windward Symmetry Plane with Surface Finite Catalytic Recombination Rates," AIAA/ASME Third Joint Thermophysics, Fluids, Plasma, and Heat Transfer Conference, AIAA Paper 82-0842, Saint Louis, MO, June 1982.

[16]Shinn, J., Moss, J. N., and Simmonds, A. L., "Viscous Shock-Layer Heating Analysis for the Shuttle Windward Symmetry Plane with Surface Finite Catalytic Recombination Rates," *Entry Vehicle Heating and Thermal Protection Systems: Space Shuttle, Solar Starprobe, Jupiter Galileo Probe,* edited by P. E. Bauer and H. E. Collicott, Vol. 85, Progress in Astronautics and Aeronautics, AIAA, New York, 1983, pp. 149–180.

[17]Veuillot, J. P., "Calcul de L'écoulement axisymétrique Autour D'un Corps de Rentrée," ONERA, Rept. RT 31/1285 AY, 1989.

[18]Adams, J. C., "Higher-Order Boundary-Layer Effects on Analytic Bodies of Revolution," Arnold Engineering Development Center, AEDC-TR-68-57, Arnold AFB, TN, April 1968.

[19]Aupoix, B., Brazier, J. Ph., Cousteix, J., and Monnoyer, F., "Second-Order Effects in Hypersonic Boundary Layers," *Third Joint Europe-US Short Course on Hypersonics—Aachen, Germany*, Oct. 1990.